Identification of a non-radiative shallow acceptor in $Zn_{0.8}Al_{0.2}O$ alloy irradiated with N^+ ion beam

Jun Kue Park[a]*, Yu-Mi Kim[a], Gi Wan Jeon[a], Weon-Sik Chae[b], and Jong-Soo Lee[c]

[a] *Particle Beam Research Division, Korea Multi-purpose Accelerator Complex, Korea Atomic Energy Research Institute (KAERI), 181 Mirae-ro, Geoncheon-eup, Gyeongju-si 38180, Republic of Korea*
[b] *Deagu Center, Korea Basic Science Institute, 80, Daehak-ro, Buk-gu, Deagu 41566, Republic of Korea*
[c] *Department of Energy Science and Engineering DGIST, 333 Techno Jungang-daero, Hyeonpung-eup, Dalseong-gun, Deagu 42988, Republic of Korea*

*Corresponding author: *jkuepark@kaeri.re.kr*

Keywords : N^+ beam irradiation, $Zn_{0.8}Al_{0.2}O$ alloy, electron spin resonance spectroscopy

1. Introduction

Zinc oxide (ZnO) is a wide band gap (Eg=3.37 eV) semiconductor material, the intrinsic n-type conductive. For ZnO, there are various applications such as cosmetics, catalysts, sensors, optical waveguide devices, and transparent conductive electrodes, and other fields. Recently, optoelectronic devices based on ZnO are an emerging subject to achieve stable and highly efficient devices. In fact, one of the long-standing problems is how to realize high-quality p-type ZnO that was a key to manufacturing ZnO-based LEDs.

The difficulties of the p-type doping may be attributed to the low solubility of acceptor impurities, self-compensation abilities of some intrinsic donor defects, and deep acceptor energy levels in ZnO. To enhance the solubility of acceptor, donor-acceptor co-doping such as N-Al, N-Ga, and Al-O bonds have been employed. In this work, we investigate on donor-acceptor pairs in Al-doped ZnO (AZO) and discuss the local electronic structures that the dopants may induce.

2. Methods

In this section, the detailed methods for N^+ beam-irradiated AZO. For the first time, we provide the activation barriers for acceptor complexes by using electron spin resonance (ESR) spectroscopy in the beam-irradiated AZO.

2.1 Sample preparation

The 30 nm-thick AZO thin films were deposited by atomic layer deposition (ALD) on p-type Si substrates with a 200 nm thick thermal oxide layer. In the ALD process, diethylzinc (DEZ, $Zn(C_2H_5)_2$), trimethyl aluminum (TMA, $Al(CH_3)_3$), and deionized water were used as precursors of Zn, Al, and oxidant, respectively. Nitrogen was used as a purge gas at a fow of 80 sccm. The process temperature of the ALD chamber was 200 ^oC.

2.2 N^+ beam irradiation

The N^+ beam irradiation was performed by using the gaseous ion beam implanter which are widely being used such as material science and condensed matter physics. The N^+ beam with the energy of 40 keV was irradiated on the samples as much as 1×10^{14}, 1×10^{15}, and 1×10^{16} ions/cm^2. The beam irradiation was performed after simulation using the SRIM package to ensure how the beam can be penetrated and straggled into the samples. According to the SRIM data, 40 keV N^+ beam may penetrate down to ~180 nm in depth.

2.3 Electron spin resonance spectroscopy

ESR measurements were performed on an X-band (~9.4 GHz) Bruker spectrometer equipped with a continuous He-flow cryostat, allowing the regulation of the sample temperature from 4 K to room temperature.

3. Results and Discussion

Figure 1(a) shows the dynamic SIMS data for N^+ exhibiting the depth profile of the nitrogen concentration. With increasing irradiation, the N+ concentration exhibits an increase with the same penetration depth. Substantial N^+ ions may be introduced in the SiO_2 layer, as well as in the AZO layer with increasing irradiation doses. In the vicinity of the interface layers, we may observe some peaks in the SIMS data.

In Fig. 1(b), the SIMS data for H^+ are displayed, in which the hydrogen is observed in the vicinity of the surface. Unexpected H^+ ions may have been introduced during the sample preparation, although H^+ beam irradiation had not been performed. For the N16 film, H^+ ion exhibits an increase compared to that of the other films. Figure 1(d) shows the XRD data for ZnO pristine as well as AZO before and after beam irradiation. For ZnO, the XRD pattern was indexed to the hexagonal wurtzite phase, with a preferential (002) crystalline orientation.

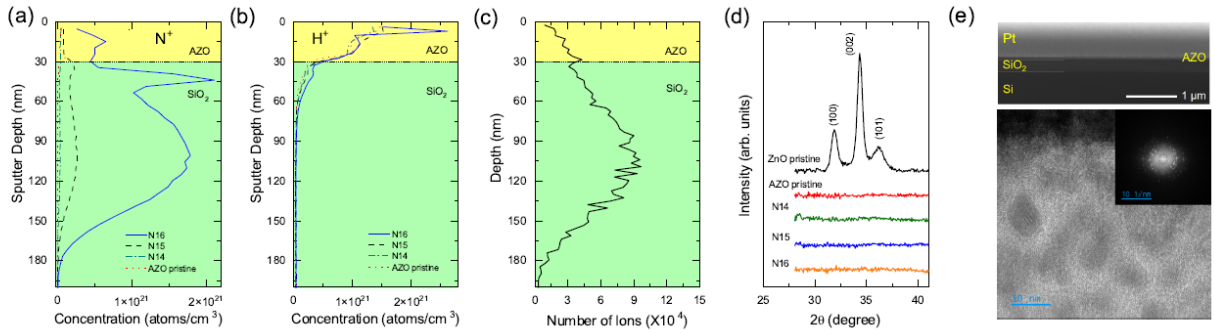

Fig. 1 Secondary ion mass spectroscopy for the AZO films (a) irradiated with N^+ beam and (b) unirradiated with H dopant. (c) SRIM simulation data for N^+ ion beam irradiated on the AZO films. (d) X-ray diffraction data for ZnO pristine, AZO pristine, and AZO irradiated with N^+ beam. (e) Cross-sectional SEM image and TEM image showing the morphologies of AZO thin films deposited by ALD.

On the other hand, all the AZO films exhibit the amorphous phase showing none of the XRD peaks. An SEM image of the cross-section of the AZO film is shown in the upper panel of Fig. 1(e), where we can obviously find the AZO layer on the SiO_2 layer. In the lower panel, HRTEM and diffraction analyses confirmed the amorphous-like nature of AZO, showing no discernible crystalline domains.

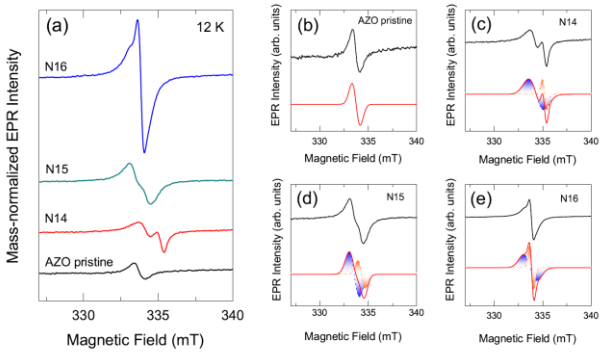

Fig. 2 Mass-normalized EPR spectra at 12 K for the AZO films before and after irradiation. Experimental ESR spectra at 12 K and simulated spectra for (b) AZO pristine, (c) N14, (d) N15, and (e) N16 films. The ESR spectra for the irradiated samples consist of two peaks.

ESR may give compatible information for the defects introduced in AZO films. In Fig. 2, mass-normalized ESR spectra before and after beam irradiation are displayed, in which the spectra after irradiation may undoubtedly exhibit two components consisting of the spectral shape, unlike in the unirradiated sample exhibiting a single resonance peak. In the N16 sample greatly increases the intensity of the ESR spectrum which may imply some defects were further introduced with a dose of 1×10^{16} ions/cm^2. In addition, with increasing irradiation doses, two resonance peaks get close to each other and thus eventually seem like one resonance peak in the N16 film [see Fig. 2(a)]. In Figs. 2(b)-2(e), the simulated spectra were well fitted to the experimental data according to the Zeeman term, giving us the fitting parameters, as summarized in Table II. The spin-Hamiltonian for the unirradiated sample only consists of a Zeeman term with a single defect, whereas that for the irradiated samples exhibits that with two kinds of defects, $\mathcal{H} = \sum_{i=1}^{2} \beta_e g_i \mathbf{S} \cdot \mathbf{B}$, where β is Bohr magnetron, g_i is the electron g-factor, **S** and **B** denote spin angular momentum operators and the applied magnetic field, respectively. To clarify whether the implanted nitrogen into SiO_2 layer may induce some defects, we perform the ESR measurement for the ZnO film irradiated with the same condition of N^+ beam with a beam energy of 40 keV and a dose of 1×10^{15} ions/cm^2. Regardless of the beam irradiation, the ZnO film does not exhibit the ESR spectra. Thus, we may exclude the ESR spectra that originated from the SiO_2 layer.

4. Conclusions

In this work, we have investigated non-radiative defects introduced by N^+ ion beam irradiation for Al-doped ZnO (AZO) films. We find that a non-radiative shallow acceptor of N_O-H-V_{Zn} can be created by N^+ ion beam irradiation in AZO alloy. In a film irradiated with a fluence of 10^{16} ions/cm^2 (N16), in particular, the non-radiative acceptor is evidenced by a newly emerged signal in electron spin resonance (ESR) spectra corresponding to a longer decay time τ in the time-resolved photoluminescence (PL). No hyperfine peaks in ESR spectra may exclude N-related acceptors and Al_{Zn} donors with a nuclear spin. The introduced acceptor complex may support the co-doping method to make ZnO p-type semiconductors.

REFERENCES

[1] J. C. Fan, K. M. Sreekanth, Z. Xie, S. L. Chang, and K. V. Rao, p-Type ZnO materials: Theory, growth, properties and devices, Prog. Mater. Sci. 58, 874-985 (2013).
[2] J. K. Park, K. W. Lee, H. Kweon, and C. E. Lee, Evidence of hydrogen-mediated ferromagnetic coupling in Mn-doped ZnO, Appl. Phys. Lett. 98, 102502 (2011).